Journal of Cell Science & Therapy

Gai , et al., J Cell Sci Ther 2017, 8:2
DOI: 10.4172/2157-7013. 1000264

Short Communication OMICS International

Protective Role of Stem Cell Derived Extracellular Vesicles in an *In Vitro* Model of Hyperglycemia-Induced Endothelial Injury

Chiara Gai[1], **Yonathan Gomez**[1], **Ciro Tetta**[2], **Maria Felice Brizzi**[1,3] **and Giovanni Camussi**[1*]

[1]*Department of Medical Sciences, University of Torino, Italy*

[2]*Unicyte AG, Oberdorf NW, Switzerland*

[3]*2i3T, Society for the Management of Enterprise Incubator and the Technology Transfer, Scarl University of Torino, Italy*

[*]**Corresponding author:** Giovanni Camussi, Department of Medical Sciences, University of Torino, Italy, Tel: +390116709588; Fax: +39 0116631184; E-mail: giovanni.camussi@unito.it

Rec date: Mar 06, 2017; **Acc date:** Mar 17, 2017; **Pub date:** Mar 20, 2017

Abstract

Background: Adipose and bone marrow derived mesenchymal stem cells are two populations of multipotent adult stem cells with immunosuppressive, anti-inflammatory, and regenerative properties. It has been previously described that extracellular vesicles (EVs) derived from stem cells possess pro-regenerative and pro-angiogenic abilities. Hyperglycemia is a pathological condition affecting diabetic patients. Long term effects of hyperglycemia are endothelial dysfunction and vascular lesions leading to diabetic microangiopathy.

The aim of the present study was to evaluate whether stem cell-derived EVs may inhibit endothelial cells dysfunction induced by hyperglycemia to mimic human microangiopathy.

Methods: We set up an *in vitro* hyperglycemic model by culturing human microvascular endothelial cells in hyperglycemic constant or intermittent conditions for 7 days, in order to mimic a chronic damage. At day 5, endothelial cells were incubated with adipose and mesenchymal stem cell-derived EVs or vehicle alone for 48 hr. At day 7, we evaluated apoptosis, oxidative stress, and capillary-like formation ability on Matrigel.

Results: Intermittent and constant high glucose models significantly decreased endothelial cell proliferation, increased number of apoptotic cells, promoted oxidation of intercellular proteins, and reduced capillary-like structure formation. Treatment with both kinds of EVs significantly restored proliferation, inhibited apoptosis and oxidation, and restored capillary-like formation.

Conclusions: The results of the present study demonstrate that adipose and bone marrow mesenchymal stem cell-derived EVs may inhibit the endothelial dysfunction induced by high glucose concentration, which mimic diabetic microvascular injury.

Keywords: Adipose stem cells; Mesenchymal stem cells; Extracellular vesicles; Human microvascular endothelial cells; Hyperglycemia; Microangiopathy; Diabetes; Angiogenesis

Abbreviations:

AKI: Acute Kidney Injury; ANGPTL1: Angiopoietin like 1; ASC: Adipose Stem Cells; EVs: Extracellular Vesicles; HES1: HES Family BHLH Transcription Factor 1; HG: Constant Hyperglycemic Model; HGF: Hepatocyte Growth Factor; HMEC: Human Microvascular Endothelial Cells; IL-8: Interleukin 8; INT HG: Intermittent Hyperglycemic Model; MFGE8: Milk Fat Globule-EGF Factor 8 protein; MMPs: Matrix Metalloproteinases; MSC: Mesenchymal Stem Cells; TCF4: Human T-cell Factor 4; TGFβ1: Transforming Growth Factor β1; v-CAM1: Vascular Cell Adhesion Molecule 1.

Introduction

Extracellular vesicles (EVs) are a heterogeneous population of vesicles, including exosomes, microvesicles, and other kind of vesicles, actively released from a wide variety of cells and commonly detectable in almost all body fluids [1]. EVs are composed by a cell membrane phospholipid bilayer which contains or encloses lipid raft-interacting proteins, surface receptors, cytoplasmic proteins, and nucleic acids. Some transmembrane proteins are common to all EVs, and are probably involved in EVs biogenesis [2], while other are cell-specific and represent a signature of the cell of origin. The nucleic acids, such as mRNA, lncRNA, miRNA, are encapsulated in EVs, at least in part through a selective mechanism, and are protected from enzymatic degradation [3-7]. In the past, few years, it has come to light that EVs play an important role in cell signaling. In fact, EVs can transfer their cargo from the cell of origin to the target cells and modify their biological activities [4-7]. EVs are able to interact with recipient cells through different mechanisms, such as direct cell stimulation, receptor-mediated endocytosis, and receptor independent mechanism. Once incorporated by cells, EVs' content can be released in the cytoplasm and mediate several biological effects [8].

Mesenchymal stem cells (MSC) are non-hematopoietic pluripotent progenitor cells present in bone marrow, umbilical cord blood, and adipose tissue and they are capable to differentiate into multiple mesoderm-, but also non-mesoderm-, cell type lineages [9]. MSC have

shown promising regenerative, immunosuppressive, and anti-inflammatory properties, so they have emerged as a potential tool for tissue repair and wound healing in regenerative medicine, but their mechanism of action is not completely understood [9]. However, it was observed that the therapeutic effects are mainly due to the paracrine mechanisms, which stimulates self-renewal and endogenous regeneration [10].

EVs have been suggested to transfer several paracrine signaling molecules, such as immunomodulators, angiogenic factors, anti-apoptotic factors, antioxidants molecules, and cellular chemotaxis inducers [11]. Recent studies showed that EVs derived from MSC (MSC EVs) contain vascular endothelial growth factor (VEGF), transforming growth factor β1 (TGFβ1), interleukin 8 (IL-8) [12,13], hepatocyte growth factor (HGF) [14-16], HES Family BHLH transcription factor 1 (HES1) [17], and human T-cell factor 4 (TCF4) [18,19], but also miRNA stimulating angiogenesis, such as miR210, miR-126, miR-132, miR-21 [20], miR-222, let-7f [21,22], and cell-cycle progression and proliferation, such as miR-191, miR-222, miR-21, let-7a [21,22].

These factors induce survival, proliferation, and proangiogenic signaling in recipient endothelial cells [11]. Adipose-derived stem cells (ASC) are mesenchymal stem cells with self-renewal property and multipotent differentiation, such as adipogenesis, osteogenesis, and chondrogenesis. Like MSC, ASC showed a promising regenerative potential in various diseases, but they became more attractive for therapeutic purposes because they can be easily isolated from subcutaneous adipose tissue [23]. Recent evidence shows that EVs derived from ASC (ASC EV) contain several angiogenic factors, such as Milk fat globule-EGF factor 8 protein (MFGE8), angiopoietin like 1 (ANGPTL1), and thrombopoietin [24]. Moreover, they carry matrix metalloproteinases (MMPs) that play an important role in angiogenesis by facilitating endothelial cell migration and by promoting activation of angiogenic growth factors and other signaling molecules [25]. It has been also shown that the proangiogenic content of ASC EVs is modulated by the microenvironment, for example *in vitro* by the addition of different growth factors [26], or *in vivo* by obesity, which reduces their pro-angiogenic potential [27].

EVs were identified as a candidate substitute for stem cells in regenerative medicine, since they can reduce safety risks, such as de-differentiation, tumorigenesis, or immune response activation due to cell transplantation [9]. Several studies have explored the regenerative properties of MSC EVs in different diseases. It was demonstrated that MSC EVs are able to reduce infarct size, to enhance tissue repair, and to increase angiogenesis in cardiovascular diseases [9].

They promote tubule-epithelial regeneration and reduction of tubular cell apoptosis, of fibrosis, and of tubular atrophy in a model of acute kidney injury (AKI) [9]. A recent study has reported that MSC EVs induce functional recovery in AKI through the transfer of miRNA [28]. MSC EVs has been shown to be effective in a model of renal ischemia reperfusion injury, with a reduction of cell apoptosis, increased proliferation and angiogenesis, amelioration of histological lesions [29]. MSC EVs can also promote wound healing, by inducing proliferation and migration of fibroblasts, and by enhancing angiogenesis, both *in vitro* [30] and *in vivo* [31].

Hyperglycemia is a major issue in diabetes mellitus and is a leading cause for the development of microangiopathy, a vascular complication that affects capillaries [32]. This pathological condition causes severe injury to microvasculature both directly and indirectly. As a consequence of an increased synthesis of growth factors, cytokines, and vasoactive agents, the vessel wall turnover is impaired and it ends in abnormal vascular remodeling [33]. Diabetic microangiopathy is characterized by impaired endothelium-dependent vasodilation, increased vessels permeability, increased prothrombotic and procoagulant activity, increased adhesion of and permeability to leucocytes, due to the rise in E-selectin and vascular cell adhesion molecule 1 (v-CAM1) levels, inflammation, increased deposition of extracellular matrix (with increased production of fibronectin and type IV collagen) [34].

Diabetic microangiopathy damages particularly renal, retinal, and neuronal capillaries, with consequent retinopathy, neuropathy, and nephropathy [34].

The aim of the present study was to evaluate the potential protective role of ASC and MSC EVs in an *in vitro* model of microvascular endothelial injury which recapitulate the chronic hyperglycemic conditions that lead to microvascular dysregulation in diabetic patients.

Materials and Methods

Cell Cultures

Human microvascular endothelial cells (HMEC) were obtained by immortalization with simian virus 40 of primary human dermal microvascular endothelial cells [35,36] and cultured as previously described [37]. HMEC cultured in normal glucose Endothelial Basal Medium (EBM, Lonza, Basel, CH) were used as control (CTR). Glucose concentration of EBM was 5.6 mM. High glucose- and high mannitol-EBM were obtained by adjusting EBM to 28 mM of α-D-glucose (Sigma Aldrich, St. Louis, MO, USA) or 28 mM of mannitol (Sigma Aldrich, St. Louis, MO, USA). Constant hyperglycemic (HG) model was performed by culturing HMEC in high glucose-EBM for 7 days. Intermittent hyperglycemic (INT HG) model was performed by culturing HMEC in 48 hour alternated cycles of high glucose-EBM, or high mannitol-EBM as osmotic control, and normal glucose-EBM, for 7 days.

Human ASC and MSC (both purchased from Lonza, Basel, CH) were cultured in Mesenchymal Stem Cell Basal Medium (MSCBM, Lonza, Basel, CH) supplemented with MSC-GM kit (Lonza, Basel, CH) and 1% Antibiotic Antimycotic solution (Sigma-Aldrich, St. Louis, MO, USA) at 37°C in 5% CO_2 incubator. ASC and MSC were grown until confluent, and sub-cultured and characterized as previously described [24,38]. Cells at passages 4 to 6 were used for the experiments.

Isolation and characterization of EVs from ASC and MSC

ASC and MSC were starved for 16 hours. Supernatants were collected and EV were isolated by differential ultracentrifugation as previously described [24]. The quality of EVs preparation was evaluated on the base of their morphology and expression of exosome markers as follow. Quantification and size distribution of EVs was performed using NanoSight LM10 (NanoSight Ltd, Minton Park, UK) equipped with nanoparticle tracking analysis NTA 2.3 analytic software [39]. Transmission electron microscopy was performed on EVs purified from MSC and ASC and observed by Jeol JEM 1010 electron microscope as previously described [2]. EVs were also characterized by Western blot analysis for the following exosomal markers: CD63, CD9, and Alix [24].

Western Blot analysis

Cells were lysed at 4°C for 20 minutes in a RIPA lysis buffer supplemented with 1% PMSF, 1% Protease Inhibitor Cocktail, 1% Phosphatase Inhibitor Cocktail 1, and 1% Phosphatase Inhibitor Cocktail 3 (all purchased by Sigma Aldrich, St. Louis, MO, USA). The lysate was centrifuged at 12,000 x g for 20 minutes at 4°C to precipitate and discard cellular debris. The protein content of the supernatants was measured by Bradford. Aliquots containing 30 µg of protein of the cell lysates were subjected to 10% sodium dodecyl sulfate-polyacrylamide gel electrophoresis under reducing conditions and electroblotted onto nitrocellulose membrane filters. The membranes were blocked with 5% nonfat milk in 20 mmol/L Tris-HCl, pH 7.5, 500 mmol/L NaCl plus 0.1% Tween (TBS-T) and immunoblotted overnight at 4°C with the relevant primary antibodies at the appropriate concentration: CD63, Alix, Actin, VEGF, v-CAM-1 (Santa Cruz Biotechnology, Dallas, TX, USA), CD9 and Fibronectin (Abcam, Cambridge, UK).

After extensive washings with TBS-T, the blots were incubated for 2 hours at room temperature with peroxidase-conjugated isotype-specific secondary antibodies (Pierce, Thermo Fisher Scientific, Waltham, MA, USA), washed with TBS-T. The protein bands were visualized with Clarity Western ECL Substrate (Bio-Rad, Hercules, CA, USA) and ChemiDoc™ XRS+ System (Bio-Rad, Hercules, CA, USA). The average density of each band was measured by Quantity One Analysis Software (Bio-Rad, Hercules, CA, USA), normalized for the average density of the respective actin band. The mean normalized density of at least 4 experiments is expressed as fold change over CTR.

Real time PCR

Total RNA was extracted by TriZol reagent (Life Technologies, Thermo Fisher Scientific, Waltham, MA, USA) according to manufacturer's instructions. cDNA was produced from total RNA using the High Capacity cDNA Reverse Transcription Kit (Applied Biosystems, Thermo Fisher Scientific, Waltham, MA, USA). Briefly, 200 ng mRNA, 2 µl RT buffer, 0.8 µl dNTP mixture, 2 µl RT random primers, 1 µl MultiScribe reverse transcriptase, and 4.2 µl nuclease-free water were used for each cDNA synthesis. Twenty microliters of RT-PCR mix, containing 1X SYBR GREEN PCR Master Mix (Applied Biosystems, Thermo Fisher Scientific, Waltham, MA, USA), 100 nM of each primer (VEGF or GAPDH), were analyzed using a 48-well StepOne Real Time System (Applied Biosystems, Thermo Fisher Scientific, Waltham, MA, USA). Negative cDNA controls (no cDNA) were cycled in parallel with each run.

BrdU proliferation assay

HMEC at 5 days of HG or INT HG conditioning were seeded at 2,000 cells/well into 96-well plates with AF in EBM medium (adjusted or not to 28 mM glucose) and left to adhere. After 4 hr, cell medium was changed with DMEM (Euroclone, Pero, MI, IT) adjusted or not to 28 mM glucose and supplemented with 10% ultra-centrifuged Fetal Bovine Serum (FBS, Thermo Fisher Scientific, Waltham, MA, USA). FBS was ultra-centrifuged for 8 hr to remove EVs. Then, cells were treated with EVs from ASC or MSC at the dose of 10,000 EVs/cell. DNA synthesis was detected as incorporation of 5-bromo-2′-deoxyuridine (BrdU) into the cellular DNA using an ELISA kit (Roche, Basel, CH), following the manufacturer's instructions. Optical density was measured with an ELISA reader (Bio-Rad, Hercules, CA, USA) at 405 nm.

Annexin V apoptosis assay

HMEC at day 5 of hyperglycemic conditioning were plated on 24-well plates at a density of 2×10^4 cells/well with AF in EBM medium (adjusted or not to 28 mM glucose) and left to adhere. Then, cell medium was changed with DMEM (Euroclone Pero, MI, IT) adjusted or not to 28 mM glucose and supplemented with 10% ultra-centrifuged Fetal Bovine Serum (FBS, Thermo Fisher Scientific, Waltham, MA, USA). Cells were treated with EVs from ASC or MSC at the dose of 10^4 EVs/cell. At day 7 of hyperglycemic conditioning, cells were washed with PBS and harvested with 1% trypsin.

Supernatant, PBS used for washing and cells were collected by centrifugation at 400 × g for 5 min. After removal of the supernatant, cells were resuspended in 100 µl of DMEM. Then 100 µl of Muse Annexin V and Dead Cell Kit reagent (Merck-Millipore, Darmstadt, D) was added to each sample, cells were mixed and incubated at RT for 20 minutes in the dark. Qualitative and quantitative assessments of apoptosis were conducted with a Muse Cell analyzer (Merck Millipore, Darmstadt, D).

Oxidative stress analysis

HMEC at day 5 of hyperglycemic conditioning were plated on 8-well chamber slides (Thermo Fisher Scientific, Waltham, MA, USA) at a density of 10^4 cells/well with AF in EBM medium (adjusted or not to 28 mM glucose) and left to adhere. Then, cell medium was changed with DMEM (Euroclone, Pero, MI, IT) adjusted or not to 28 mM glucose and supplemented with 10% ultra-centrifuged FBS (Thermo Fisher Scientific, Waltham, MA, USA). Cells were treated with EVs from ASC or MSC at the dose of 10^4 EVs/cell. At day 7 of hyperglycemic conditioning, cells were washed with PBS, fixed with ice-cold methanol and protein carbonyls generated by oxidative stress were labelled with 2,4-dinitrophenylhydrazine (DNPH) from OxyICC kit (Merck Millipore, Darmstadt, D), according with manufacturer's instructions.

DNPH was detected by a peroxidase-conjugated antibody and streptavidin was used as substrate. Nuclei were stained with DAPI. All reagents were provided by OxyICC kit (Merck Millipore, Darmstadt, D). The immunodetection was performed by a fluorescent confocal microscope (Zeiss, Oberkochen, D) at 60x magnification. Fluorescence intensity was measured by ImageJ 1.49v software (NIH) and corrected total cell fluorescence (CTCF) was calculated as previously described [40,41].

In vitro angiogenic assay

In vitro formation of capillary-like structures was studied on growth factor-reduced Matrigel (Corning, Tewksbury, MA, USA). To evaluate the formation of capillary-like structures, HMEC were washed twice with phosphate-buffered saline, detached with 1% trypsin, and seeded (2×10^4 cells/well) onto Matrigel-coated wells in DMEM supplemented with 10% ultra-centrifuged FBS and adjusted or not to 28 mM of glucose, in the presence or absence of EVs from ASC or MSC (10^4 EVs/cell). After 24 hr, cells were observed with a Nikon-inverted microscope (10X), and photographed with a Leica-digital camera. Image analysis was performed automatically with the Angiogenesis Analyzer tool by ImageJ 1.49v software (NIH).

Statistical analysis

Statistical analysis was performed using GraphPad Prism 6.01 Software. Proliferation (BrdU), apoptosis (Annexin V), oxidative stress (DNPH), and tube formation assay (Matrigel) were analyzed using Ordinary One Way Anova test, significance was calculated by Fisher's LSD test. Western Blot data were analyzed using nonparametric Kruskal-Wallis test.

For Real Time PCR data analysis, Excel software (Microsoft Office 365 ProPlus) was used to calculate ΔCt, -ΔΔCt, and RQ. Statistical analysis was performed on RQ values by GraphPad Prism 6.01 software using nonparametric Kruskal-Wallis test. We considered differences to be statistically significant when $p<0.05$. At least 4 experiments for each assay were performed with similar results. Data are expressed as mean ± SEM.

Results and Discussion

As shown in Figure 1 EVs released from ASC and MSC showed comparable size and concentration as seen by NanoSight. The size was similar also by transmission electron microscopy, but ASC EVs were less homogeneous then MSC EVs (Figure 1). By western blot both EVs expressed the exosome marker CD63.

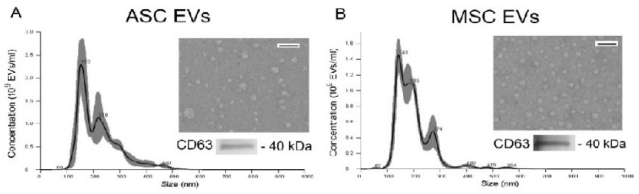

Figure 1: Characterization of ASC and MSC EVs. Representative NanoSight analysis of ASC EVs (A) and MSC (B) EVs showing concentration of particles (109 EVs/ml) and size (nm). Insets show transmission electron microscopy of EVs negatively stained with NanoVan. EVs were viewed using a JEOL Jem 1010 electron microscope (original magnification × 75,000, black line=200 nm). Representative western blot analysis of EVs purified by differential ultracentrifugation showing the expression of the exosome marker CD63.

In order to test the protective role of stem cell derived EVs, we set up an *in vitro* hyperglycemic model of endothelial injury. We chose to condition cells with a glucose level comparable to glycemic concentration measurable in diabetic patients. Cells were conditioned for 7 days in order to mimic a chronic damage. HMEC were cultured in constant high glucose (HG), or in intermittent high glucose (INT HG), which mimic glucose peaks occurring in diabetic patients.

Figure 2A shows the experimental condition. HMEC cultured with a normal glucose concentration were used as control (CTR) and HMEC cultured with constant high mannitol (HM) concentration were used as osmotic control. HMEC were treated with EVs at day 5.

As shown in Figures 2C and 2D, differences in the expression of some endothelial marker were observed after hyperglycemic conditioning. Western blot analysis showed significantly higher level of fibronectin (Figure 2C) and v-CAM1 (Figure 2D) protein in both HG and INT HG conditions compared to CTR.

Fibronectin is a glycoprotein of the extracellular matrix that binds to integrins and plays a major role in cell adhesion, growth, migration, and in wound healing. Increased fibronectin expression is associated with fibrosis and endothelial inflammation [42].

v-CAM1 is a vascular cell adhesion protein which mediates the adhesion of lymphocytes, monocytes, eosinophils and basophils to vascular endothelium. Up-regulation of v-CAM1 in endothelial cells is associated to the development of atherosclerosis and endothelial inflammation [43]. Therefore, the up-regulation of these proteins indicates that both HG and INT HG conditionings induced an inflammatory phenotype on endothelial cells.

On the contrary, VEGF protein level was significantly lower in HMEC in HG and INT HG conditions, compared to NG condition (Figure 2E). This was confirmed by Real Time PCR, which showed a reduction in the transcript of VEGF-A isoform in HG condition and a significant reduction in INT HG condition, compared to CTR (Figure 2B).

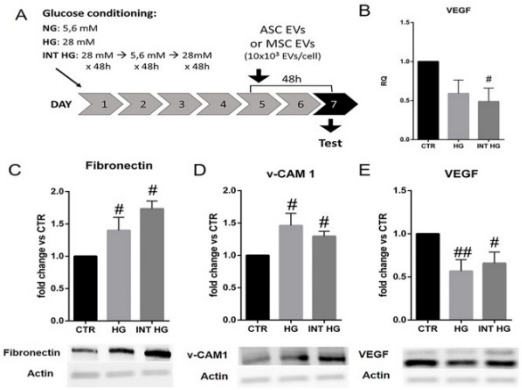

Figure 2: set up of *in vitro* hyperglycemic model of endothelial injury. The scheme summarizes glucose concentration and time points of cell conditioning with high glucose media for setting up the model and dose and time of EVs treatment (A). Real Time PCR for VEGF transcript in both HG and INT HG conditions is expressed as Relative Quantification (RQ) on CTR. GAPDH was used as endogenous control (B). Representative western blot for fibronectin (C), v-CAM1 (D), and VEGF (E) are shown. The intensity of each band was quantified and normalized for Actin. The mean of $n \geq 4$ experiments is shown and expressed as fold change vs CTR. All histograms represent mean ± SEM. # $p \leq 0.05$ and ## $p \leq 0.01$ for HG/INT HG vs CTR.

VEGF is a signal protein that stimulates vasculogenesis and angiogenesis. Evidence shows that VEGF is down-regulated in endothelial cells in hyperglycemic conditions and this stimulate cell apoptosis [44]. Moreover, VEGF reduction may lead to reduced vessel-structure formation ability and increased apoptosis.

Thus, both HG and INT HG models were able to damage endothelial cells and were a suitable *in vitro* model of hyperglycemic injury.

Then, we performed proliferation and apoptosis assays to understand whether high glucose affects proliferation and survival of endothelial cells and whether ASC and MSC EVs exert a protective role from high glucose damages. As shown in Figure 3, BrdU

incorporation in dividing cells was significantly reduced in both HG (Figure 3A) and INT HG (Figure 3B) conditions, compared to CTR.

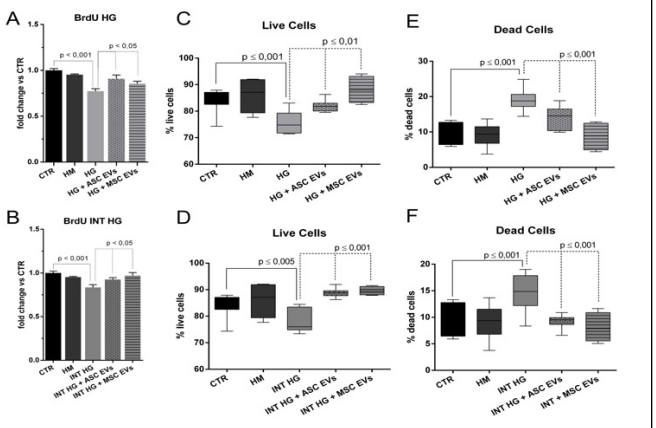

Figure 3: pro-proliferative and anti-apoptotic effects of ASC and MSC EVs BrdU proliferation assay for HG (A) and INT HG (B) models. Histograms (A, B) shows mean ± SEM of n=5 experiments expressed as fold change vs CTR. Annexin V apoptosis assay (C-F) showed the percentage of live cells in HG (C) and INT HG (D) models and also percentage of dead cells in HG (E) and INT HG (F) models. The boxes in plots (C-F) show 10-90 percentile, whiskers represent min to max value; n=4 experiments were performed for each data-set. The statistical significance was calculated comparing HG/INT HG vs CTR and HG/INT HG+EVs vs HG/INT HG.

After a 48 hr treatment with ASC and MSC EVs, the proliferation was significantly increased in both HG (Figure 3A) and INT HG (Figure 3B) conditions compared to untreated HG- or INT HG-conditioned cells. EVs from ASC were less effective then MSC EVs (Figures 3A and 3B). Proliferation was not affected by HM conditioning.

By Annexin V apoptosis assay, we observed that the percentage of living cells was significantly reduced in HG condition compared to CTR. EVs showed a protective effect (Figure 3C). The percentage of dead cells was also significantly increased in HG condition, and reduced after EVs treatment.

EVs from MSC showed a stronger anti-apoptotic effect compared to ASC EVs (Figure 3D). Also in INT HG model, the percentage of live cells was significantly reduced (Figure 3E) and the percentage of dead cells was significantly increased (Figure 3F). Treatment with both ASC and MSC EVs significantly reverted INT HG effects (Figures 3E and 3F) compared to untreated INT HG cells. In the INT HG model the anti-apoptotic potential of the two types of EVs was comparable.

These results indicate that ASC and MSC EVs antagonized high glucose effects on endothelial cells by promoting proliferation and inhibiting cells death. When compared, the two sources of EVs those derived from MSC were more effective.

Another sign of cells injury induced by high glucose concentration is the oxidative stress, with the formation of free radicals leading to protein oxidation. Thus, we evaluated the levels of oxidized proteins in the hyperglycemic model. We observed that the oxidative stress was remarkably increased in HG (Figure 4C) and INT HG (Figure 4D) but not HM (Figure 4B) conditions compared to CTR (Figure 4). The quantitative analysis of cell fluorescence intensity (CTCF) confirmed that the increased protein oxidation was statistically significant in both HG (Figure 4I) and INT HG (Figure 4J) conditions.

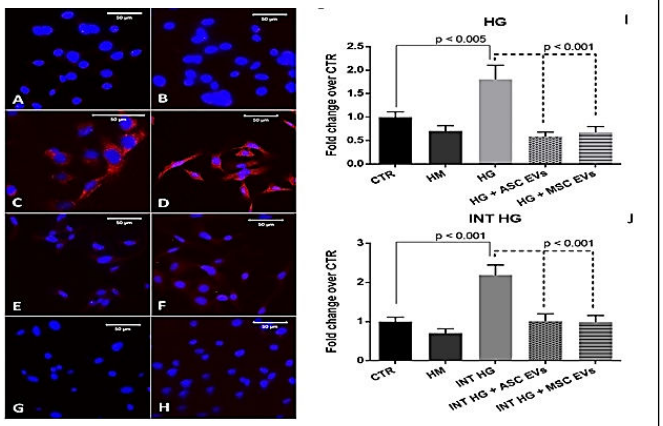

Figure 4: anti-oxidant activity of ASC and MSC EVs. Representative images of immunofluorescent staining of nuclei with DAPI (blue) and oxidized proteins with 2,4-DNPH (red) of CTR (A), HM (B), HG (C), INT HG (D), HG+ASC EVs (E), INT HG+ASC EVs (F), HG+MSC EVs (G), INT HG+MSC EVs (H). Scale bars in the upper-right corner of each photograph indicate 50 μm. Pictures were taken by Zeiss fluorescent confocal microscope at 60x magnification. Histograms show the mean CTCF ± SEM expressed as fold change over CTR for HG (I) and INT HG (J) models. N=4 experiments were performed for each data set. The statistical significance was calculated comparing HG/INT HG vs CTR and HG/INT HG+EVs vs HG/INT HG.

After the treatment with ASC (Figures 4E and 4F) and MSC (Figures 4G and 4H) EVs, we observed a significant decrease of the oxidative stress in both hyperglycemic conditions. The measurement of the mean fluorescence intensity confirmed that the reduction of oxidized protein after EVs treatment was statistically significant in both HG (Figure 4I) and INT HG (Figure 4J) models. This data suggests that EVs may play an anti-oxidant role. Consistent with our previous data [45] the present data suggest that EVs may play an anti-oxidant role.

Moreover, we investigated the capability of endothelial cells to form capillary-like structures in high glucose conditions in Matrigel. In fact, HMEC in CTR (Figure 5A) and HM (Figure 5B) spontaneously form vessel like structures. We observed that HMEC in HG (Figure 5C) and INT HG (Figure 5D) partially lost this ability. In both HG and INT HG conditions, total length of capillary-like structures was significantly reduced compared to CTR, while HM condition was comparable to CTR.

As shown in Figure 5, the treatment with ASC and MSC EVs significantly increased the number of vessel-like structures in both HG and INT HG models. This confirms that ASC and MSC EVs have both pro-angiogenic properties [11,24] and are able to restore tube formation ability in endothelial cells damaged by high glucose conditioning. These biological effects are consistent with previous observation that MSC EVs and ASC EVs contain several pro-angiogenic factors [11-14,24-27] and miRNAs [20-22,46].

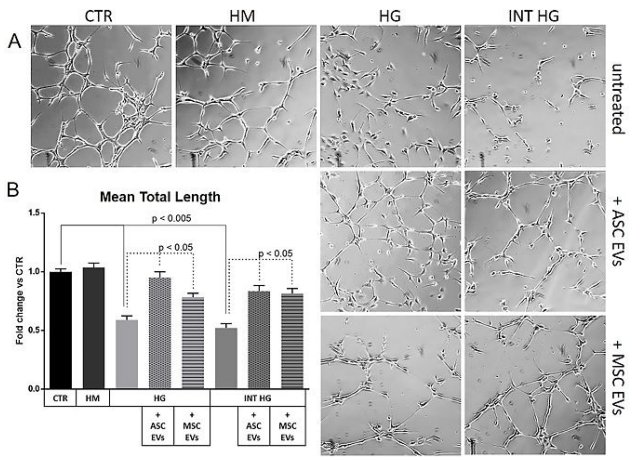

Figure 5: Pro-angiogenic activity of ASC and MSC EVs. Representative images of capillary-like structures formed by HMEC seeded on Matrigel-coated plates in different conditions: CTR, HM, HG, INT HG, HG+ASC EVs, INT HG+ASC EVs, HG+MSC EVs, INT HG+MSC EVs (A). Pictures were taken by a Leica camera installed on a Nikon inverted microscope at 10x magnification. Histograms show the mean total length ± SEM expressed as fold change over CTR for HG and INT HG models (B). N=4 experiments were performed for each data set. The statistical significance was calculated comparing HG/INT HG vs CTR and HG/INT HG+EVs vs HG/INT HG.

Conclusion

In conclusion, our work shows that ASC and MSC EVs both exert regenerative effects in a hyperglycemic model mimicking microangiopathy conditions occurring in diabetic patients. They promote endothelial proliferation and survival contrasting hyperglycemia-induced injury. In addition, by inhibiting oxidation of endothelial proteins and by promoting angiogenesis, EVs may reduce the pro-inflammatory effect of hyperglycemia [33,42-44] and the impaired angiogenesis [34].

Acknowledgements

This work was supported by a Grant from Unicyte AG, Oberdorf NW, Switzerland.

References

1. Xu R, Greening DW, Zhu HJ, Takahashi N, Simpson RJ (2016) Extracellular vesicle isolation and characterization: Toward clinical application. J Clin Invest 126: 1152-1162.
2. Iavello A, Frech VS, Gai C, Deregibus MC, Quesenberry PJ, et al. (2016) Role of Alix in miRNA packaging during extracellular vesicle biogenesis. Int J Mol Med 37: 958-966.
3. Collino F, Deregibus MC, Bruno S, Sterpone L, Aghemo G, et al. (2010) Microvesicles derived from adult human bone marrow and tissue specific mesenchymal stem cells shuttle selected pattern of miRNAs. PLoS ONE 5: e11803.
4. Ratajczak J, Miekus K, Kucia M, Zhang J, Reca R, et al. (2006) Embryonic stem cell-derived microvesicles reprogram hematopoietic progenitors: Evidence for horizontal transfer of mRNA and protein delivery. Leukemia 20: 847-856.
5. Deregibus MC, Cantaluppi V, Calogero R, Lo Iacono M, Tetta C, et al. (2007) Endothelial progenitor cell derived microvesicles activate an angiogenic program in endothelial cells by a horizontal transfer of mRNA. Blood 110: 2440-2448.
6. Valadi H, Ekström K, Bossios A, Sjöstrand M, Lee JJ, et al. (2007) Exosome-mediated transfer of mRNAs and microRNAs is a novel mechanism of genetic exchange between cells. Nat Cell Biol 9: 654-659.
7. Balaj L, Lessard R, Dai L, Cho YJ, Pomeroy SL, et al. (2011) Tumour microvesicles contain retrotransposon elements and amplified oncogene sequences. Nat Commun 2: 180.
8. Gai C, Carpanetto A, Deregibus MC, Camussi G (2016) Extracellular vesicle-mediated modulation of angiogenesis. Histol Histopathol 31: 379-391.
9. Rani S, Ryan AE, Griffin MD, Ritter T (2015) Mesenchymal stem cell-derived extracellular vesiscles: Toward cell-free therapeutic applications. Mol Ther 23: 812-823.
10. Biancone L, Bruno S, Deregibus MC, Tetta C, Camussi G (2012) Therapeutic potential of mesenchymal stem cell-derived microvesicles. Nephrol Dial Transplant 27: 3037-3042.
11. Merino-González C, Zuñiga FA, Escudero C, Ormazabal V, Reyes C, et al. (2016) Mesenchymal stem cell-derived extracellular vesicles promote angiogenesis: Potential clinical application. Front Physiol 7: 24.
12. Coultas L, Chawengsaksophak K, Rossant J (2005) Endothelial cells and VEGF in vascular development. Nature 438: 937-945.
13. Olsson AK, Dimberg A, Kreuger J, Claesson-Welsh L (2006) VEGF receptor signaling-In control of vascular function. Nat Rev Mol Cell Biol 7: 359-371.
14. Morishita R, Nakamura S, Hayashi SI, Taniyama Y, Moriguchi A, et al. (1999). Therapeutic angiogenesis induced by human recombinant hepatocyte growth factor in rabbit hind limb ischemia model as cytokine supplement therapy. Hypertension 33: 1379–1384.
15. Chade AR, Stewart N (2013) Angiogenic cytokines in renovascular disease: Do they have potential for therapeutic use? J Am Soc Hypertens 7: 180-190.
16. Tan CY, Lai RC, Wong W, Dan YY, Lim SK, et al. (2014) Mesenchymal stem cell-derived exosomes promote hepatic regeneration in drug-induced liver injury models. Stem Cell Res Ther 5: 76.
17. Kitagawa M, Hojo M, Imayoshi I, Goto M, Ando M, et al. (2013) Hes1 and Hes5 regulate vascular remodeling and arterial specification of endothelial cells in brain vascular development. Mech Dev 130: 458-466.
18. Maruotti N, Corrado A, Neve A, Cantatore FP (2013) Systemic effects of Wnt signaling. J Cell Physiol 228: 1428-1432.
19. Lu R, Qu Y, Ge J, Zhang L, Su Z, et al. (2012) Transcription factor TCF4 maintains the properties of human corneal epithelial stem cells. Stem Cells 30: 753-761.
20. Chen TS, Lai RC, Lee MM, Choo ABH, Lee CN, et al. (2010) Mesenchymal stem cell secretes microparticles enriched in pre-microRNAs. Nucleic Acids Res 38: 215-224.
21. Yoo JK, Kim J, Choi SJ, Noh HM, Kwon YD, et al. (2011) Discovery and characterization of novel microRNAs during endothelial differentiation of human embryonic stem cells. Stem Cells Dev 21: 2049-2057.
22. Nagpal N, Kulshreshtha R (2014) miR-191: An emerging player in disease biology. Front Genet 5: 99.
23. Dai R, Wang Z, Samanipour R, Koo KI, Kim K (2016) Adipose-derived stem cells for tissue engineering and regenerative medicine applications. Stem Cells Int: 6737345.
24. Lopatina T, Bruno S, Tetta C, Kalinina N, Porta M et al. (2014) Platelet-derived growth factor regulates the secretion of extracellular vesicles by adipose mesenchymal stem cells and enhances their angiogenic potential. Cell Commun Signal 12: 26.
25. Lee JK, Park SR, Jung BK, Jeon YK, Lee YS, et al. (2013) Exosomes derived from mesenchymal stem cells suppress angiogenesis by down-regulating VEGF expression in breast cancer cells. PLoS ONE 8: e84256.

26. Lopatina T, Mazzeo A, Bruno S, Tetta C, Kalinina N, et al. (2014) The angiogenic potential of adipose mesenchymal stem cell-derived extracellular vesicles is modulated by basic fibroblast growth factor. J Stem Cell Res Ther 4: 245.
27. Togliatto G, Dentelli P, Gili M, Gallo S, Deregibus C, et al. (2016) Obesity reduces the pro-angiogenic potential of adipose tissue stem cell-derived extracellular vesicles (EVs) by impairing miR-126 content: Impact on clinical applications. Int J Obes (Lond) 40: 102-111.
28. Collino F, Bruno S, Incarnato D, Dettori D, Neri F, et al. (2015) AKI Recovery induced by mesenchymal stromal cell-derived extracellular vesicles carrying microRNAs. JASN 26: 2349-2360.
29. Zou X, Gu D, Xing X, Cheng Z, Gong D, et al. (2016) Human mesenchymal stromal cell-derived extracellular vesicles alleviate renal ischemic reperfusion injury and enhance angiogenesis in rats. Am J Transl Res 8: 4289-4299.
30. Shabbir A, Cox A, Rodriguez-Menocal L, Salgado M, Badiavas EV (2015) Mesenchymal stem cell exosomes induce proliferation and migration of normal and chronic wound fibroblasts, and enhance angiogenesis *in vitro*. Stem Cells and Dev 24: 1635-1647.
31. Zhang J, Guan J, Niu X, Hu G, Guo S, et al. (2015). Exosomes released from human induced pluripotent stem cells-derived MSCs facilitate cutaneous wound healing by promoting collagen synthesis and angiogenesis. J Transl Med 13: 49.
32. Perrin RM, Harper SJ, Bates DO (2007) A role for the endothelial glycocalyx in regulating microvascular permeability in Diabetes Mellitus. Cell Biochem Biophys 49: 65-72.
33. di Mario U, Pugliese G (2003) Pathogenetic mechanisms of diabetic microangiopathy. International Congress Series 1253: 171-182.
34. Schalkwijk CG, Stehouwer CDA (2005) Vascular complications in Diabetes Mellitus: the role of endothelial dysfunction. Clin Sci (Lond) 109: 143-159.
35. Ades WE, Candal FJ, Swerlick RA, George VG, Summers S, et al. (1992) HMEC-1: Establishment of an immortalized human microvascular endothelial cell line. J Invest Dermatol 99: 683.
36. Xu Y, Swerlick RA, Sepp N, Bosse D, Ades EW, et al. (1994) Characterization of expression and modulation of cell adhesion molecules on an immortalized human dermal microvascular endothelial cell line (HMEC-1). J Invest Dermatol 102: 833.
37. Zanone MM, Favaro E, Conaldi PG, Greening J, Bottelli A, et al. (2003) Persistent infection of human microvascular endothelial cells by coxsackie B viruses induces increased expression of adhesion molecules. J Immunol 171: 438-446.
38. Kuhbier JW, Weyand B, Radtke C, Vogt PM, Kasper C, et al. (2010) Isolation, characterization, differentiation, and application of adipose-derived stem cells. Adv Biochem Eng Biotechnol 123: 55-105.
39. Dragovic RA, Gardiner C, Brooks AS, Tannetta DS, Ferguson DJ, et al. (2011) Sizing and phenotyping of cellular vesicles using nanoparticle tracking analysis. Nanomedicine 7(6): 780-788.
40. Burgess A, Vigneron S, Brioudes E, Labbé J-C, Lorca T, et al. (2010) Loss of human Greatwall results in G2 arrest and multiple mitotic defects due to deregulation of the cyclin B-Cdc2/PP2A balance. Proc Natl Acad Sci USA 107: 12564-12569.
41. McCloy RA, Rogers S, Caldon CE, Lorca T, Castro A, et al. (2014) Partial inhibition of Cdk1 in G 2 phase overrides the SAC and decouples mitotic events. Cell Cycle 13: 1400-1412.
42. Feaver RE, Gelfand BD, Wang C, Schwartz MA, Blackman BR (2010) Atheroprone hemodynamics regulate fibronectin deposition to create positive feedback that sustains endothelial inflammation. Circ Res 106: 1703-1711.
43. Verginelli F, Adesso L, Limon I, Alisi A, Gueguen M, et al. (2015) Activation of an endothelial Notch1-Jagged1 circuit induces VCAM1 expression, an effect amplified by interleukin-1β. Oncotarget 6: 43216-43229.
44. Yang Z, Mo X, Gong Q, Pan Q, Yang X, et al. (2008) Critical effect of VEGF in the process of endothelial cell apoptosis induced by high glucose. Apoptosis. 13: 1331-1343.
45. Gallo S, Gili M, Lombardo G, Rossetti A, Rosso A, et al. (2016) Stem cell-derived, microrna-carrying extracellular vesicles: A novel approach to interfering with mesangial cell collagen production in a hyperglycaemic setting. PLoS One 11: e0162417.
46. Collino F, Pomatto M, Bruno S, Lindoso RS, Tapparo M, et al. (2017) Exosome and microvesicle-enriched fractions isolated from mesenchymal stem cells by gradient separation showed different molecular signatures and functions on renal tubular epithelial cells. Stem Cell Rev.